# Head morphology of the duckbill eel, *Hoplunnis punctata* (Regan, 1915; Nettastomatidae: Anguilliformes) in relation to jaw elongation

Soheil Eagderi [a,b,*], Dominique Adriaens [a]

[a] *Evolutionary Morphology of Vertebrates, Ghent University, K.L. Ledeganckstraat 35, B-9000 Ghent, Belgium*
[b] *Department of Fisheries and Environmental Sciences, Faculty of Natural Resources, Tehran University, Karaj, Iran*

## ARTICLE INFO

## ABSTRACT

*Hoplunnis punctata*, a member of the Anguilliformes, is a long-snouted eel that lives in benthic habitats of the continental shelf of tropical waters. The purpose of this study was to examine the skull morphology of this little known nettastomatid and to understand the changes associated with jaw elongation as well as the implications of jaw elongation on the feeding apparatus. We present a detailed description of the cranial osteology and myology of *H. punctata* and how these characters differ from *Conger conger* (Congrinae: Congridae), a representative with moderate jaw length, and *Heteroconger hassi* (Heterocongrinae: Congridae), a representative with a short jaw. Shape comparison shows a caudal displacement of the hyomandibula, quadrate–mandibular articulation and opercle–hyomandibular joint, decrease in the depth of the neurocranium, and increase in the distance between the anterior suspensorial facet and the posterior end of the orbit in *H. punctata* as a result of jaw elongation. These characteristics along with its immobile, long maxillary and well-developed adductor mandibulae muscle complex suggest that food may be obtained by powerful biting. Jaw elongation potentially affects the functioning of the feeding apparatus in *H. punctata* by providing more space for the olfactory rosette, increasing biting speed and reducing drag during prey capture.

© 2010 Elsevier GmbH. All rights reserved.

## 1. Introduction

The evolution of the feeding system in fishes has been the subject of many functional morphology studies (Lauder, 1982; Ferry-Graham and Lauder, 2001; Wilga, 2005; Westneat, 2004; Wainwright et al., 2007). Differences in feeding mode may be reflected in different morphological specializations of the head in relation to different functional demands (Wainwright and Bellwood, 2002). A morphological comparative analysis of the cephalic region in its proper phylogenetic context can then allow a better understanding of the morphological changes leading to extensive morphological specialization. This may then also allow a better understanding of the implications of the performance as changes occur. One aspect related to this is the elongation of the rostral region and jaw, which originated as the result of a convergent evolution among many teleost lineages (Westneat, 2004). The anguilliform fishes have adapted to diverse life styles, which

may be linked to the wide range of cranial forms (Verraes, 1981). This cranial variation, with associated muscles, can be expected to largely reflect evolutionary patterns of feeding specialization in the Anguilliformes. We use an evolutionary perspective to compare the feeding apparatus of three species of the anguilliforms to better understand the changes involved in the elongation of the rostral region and jaws.

The Nettastomatidae or duck bill eels are a group of long-snouted eels mainly found on the outer continental shelf and continental slope of the tropics. Little is known about their biology, except for their benthic habits. They are non-burrowing or crevice-dwelling eels, feeding on a variety of small fishes and invertebrates (Smith, 1989a).

This study was conducted to understand the morphological peculiarities of the skull associated with the rostral region and jaw elongation and the resulting implications for the feeding apparatus in the duckbill eel, *Hoplunnis punctata*. We provide a detailed description of the cranial osteology and myology of *H. punctata* (with the snout length ($S$) = 34–38% of the head length (HL)) and its differences with respect to representatives of two closely related anguilliform subfamilies: *Conger conger* (Congrinae: Congridae), with a moderate jaw length ($S$ = 22–27% of HL); and *Heteroconger hassi* (Heterocongrinae: Congridae), with a short jaw length

* Corresponding author at: Biology Department, Evolutionary Morphology of Vertebrates, Ghent University, K.L. Ledeganckstraat 35, B-9000 Ghent, Belgium. Tel.: +32 9 264 52 33.
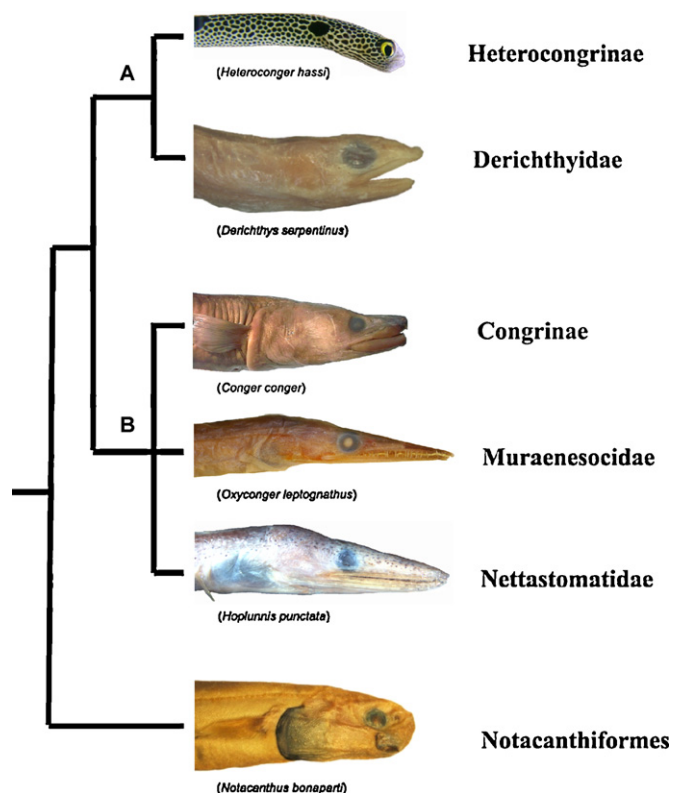*E-mail address:* soheil.eagderi@yahoo.com (S. Eagderi).

**Fig. 1.** Phylogeny of the taxa considered in this study, based on mitochondrial 12S ribosomal RNA and mtDNA sequences (modified after Wang et al., 2003).

($S$ = 11–13% of HL). The Nettastomatidae form a monophyletic group with the Congrinae, Muraenesocidae, Heterocongrinae and Derichthyidae, and the Notacanthiformes, a closely related elopomorph taxon with a short jaw, is considered an outgroup (Wang et al., 2003; Fig. 1).

## 2. Material and methods

For anatomical descriptions, five alcohol-preserved specimens of *H. punctata* obtained from the Musée National d'Histoire Naturel of Paris (MNHN 1965-0649) and the Florida Museum of Natural History (UF 216386) were examined. The specimens were of the following sizes: HP1: standard length (SL) = 365 mm (MNHN); HP2: SL = 314 mm (MNHN); HP3: SL = 311 mm (MNHN); HP4: SL = 598 mm (UF) and HP5: SL = 531 mm (UF).

Two specimens were cleared and stained according to the protocol of Hanken and Wassersug (1981) for studying the osteology. For the dissections, muscle fibers were stained according to Bock and Shear (1972). Specimens were studied using a stereoscopic microscope (Olympus SZX-7; Olympus, Tokyo, Japan) equipped with a camera lucida. Strictly for visualization purposes, the overall shape differences observed between the skulls of three species are presented as deformation grids using tpsSpline (version 1.16; Rohlf, 2004a). For this purpose, 11 landmarks (Table 1) were digitized on one specimen of each species using tpsDig (version 2.08; Rohlf, 2005). The package tpsUtil (version 1.26; Rohlf, 2004b) was used to generate the required tps file. The specimens used were from the Zoological Museum of the Ghent University (*C. conger*; UGMD 53065) and 3D pictures of *H. hassi* provided by De Schepper (2007).

The terminology of cranial bones follows Böhlke (1989). The terminology for the anterior and posterior ceratohyal follows De Schepper et al. (2005). The frequently used terminology ceratohyal and epihyal is not used here because it suggests incorrect homologies. Musculature terminology follows Winterbottom (1974) and

**Table 1**
Definition of landmarks used for the shape analysis on the skull.

| Number | Definition of landmark |
|---|---|
| 1 | The anteriormost end of the rostral region |
| 2 | The anterior end of the maxilla |
| 3 | The anteriormost end of the interorbital space |
| 4 | The anterodorsal end of the basisphenoid which contacts the frontal in the posterior wall of the orbit |
| 5 | The anterior end of the pterotic bone |
| 6 | The contact point of the frontal with the anterior end of the contact line of two parietals |
| 7 | The posterodorsal end of the neurocranium |
| 8 | The anterior suspensorial articulation |
| 9 | Operculo–hyomandibular articulation |
| 10 | Quadrate–mandibular joint |
| 11 | The posteriormost end of the maxilla |

De Schepper et al. (2005). The cranial osteology and myology of *H. hassi* and *C. conger* have already been described by De Schepper et al. (2007) and De Schepper (2007), respectively.

## 3. Results

### 3.1. Cranial osteology: H. punctata

The neurocranium is elongated with a forward prolongation of the premaxillo-ethmovomeral complex, which consists of the premaxillary, ethmoid and pars vomeralis (Fig. 2). The olfactory organ of *H. punctata* fills the long olfactory fossa, which is spread almost over the entire preorbital region. The pars vomeralis of the premaxillo-ethmovomeral complex laterally forms a crest to which the anterodorsal edge of the palatopterygoid is connected. The pars vomeralis of the premaxillo-ethmovomeral complex bears one row of enlarged, strongly pointed piercing teeth (Fig. 2B and 3A).

The orbital region is composed of the frontal, basisphenoid, pterosphenoids and parasphenoid. The frontals have fused and bear a ridge at the midline (Fig. 2A). The fused frontal expands laterally creating shelves over the orbits. The anterolateral corners of these shelves are pointed forward and each bears two pores for the supraorbital canal (Fig. 2A). The frontal encloses the opening of the temporal canal at the level of the posterodorsal margin of the
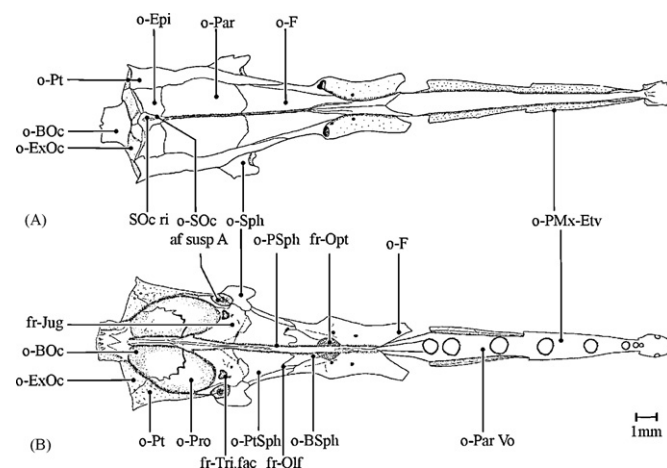


**Fig. 2.** Neurocranial bones of *Hoplunnis punctata*. (A) Dorsal view, (B) ventral view. *Abbreviations*: af susp A, anterior suspensorial articulation facet; fr-Jug, foramen jugularis; fr-Opt, foramen opticum; fr-Olf, foramen olfactorius; fr-Tri.fac, foramen trigemino-facialis; o-BOc, basioccipital; o-BSph, basisphenoid; o-Epi, epiotic (epi-occipital); o-ExOc, exoccipital; o-F, frontal; o-Par, parietal; o-Par Vo, pars vomeralis of premaxillo-ethmovomeral complex; o-PMx-Etv, premaxillo-ethmovomeral complex; o-Pro, prootic; o-PSph, parasphenoid; o-Pt, pterotic; o-PtSph, pterosphenoid; o-SOc, supraoccipital; o-Sph, sphenotic; SOc ri, supraoccipital ridge.
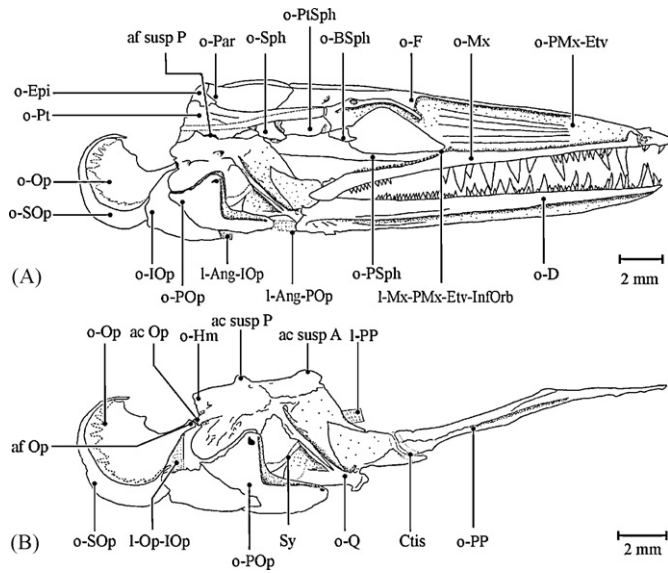
**Fig. 3.** Cranial skeleton of *H. punctata* (lateral view). (A) Complete skull (right side), (B) suspensorium (right side). *Abbreviations*: ac Op, opercular articular condyle; af Op, opercular articular facet; ac susp A, anterior suspensorial condyle; ac susp P, posterior suspensorial condyle; af susp P, posterior suspensorial articulation facet; Ctis, connective tissue; l-Ang-IOp, angulo-interopercular ligament; l-Ang-POp, angulo-preopercular ligament; l-Mx-PMx-Etv-InfOrb, maxillo-premaxillo-ethmovomero-infraorbital ligament; l-Op-IOp, operculo-interopercular ligament; l-PP, palatopterygoidal ligament; o-BSph, basisphenoid; o-D, dentary; o-Epi, epiotic (epioccipital); o-F, frontal; o-Hm, hyomandibula; o-IOp, interopercle; o-Mx, maxillary; o-Op, opercle; o-Par, parietal; o-PMx-Etv, premaxillo-ethmovomeral complex; o-POp, preopercle; o-PP, palatopterygoid; o-PSph, parasphenoid; o-Pt, pterotic; o-PtSph, pterosphenoid; o-Q, quadrate; o-SOp, subopercle; o-Sph, sphenotic; Sy, cartilaginous pars symplectic.

orbits (Fig. 2A). The unpaired basisphenoid has a process that barely extends into the orbit (Fig. 3A). The well-developed optic foramen is present between the basisphenoid and the frontal (Fig. 2B). The pterosphenoids form the lateroposterior part of the postorbital region. The pterosphenoid is attached to the basisphenoid, parasphenoid, sphenotic, pterotic and frontal. The olfactory foramen is present between the pterosphenoid and basisphenoid (Fig. 2B). The parasphenoid, which is connected to the basisphenoid, is a long shaft of bone that extends from the toothed pars vomeralis of the premaxillo-ethmovomeral complex up to the basioccipital. It forms

the ventral surface of the neurocranium and is narrow under the orbits.

The otic region comprises the pterotics, sphenotics, parietal, prootics and epiotics (epioccipitals sensu Patterson, 1975). The pterotics form the major lateral longitudal brace of the skull and comprise two parts. The superficial portion is tubular and is anteriorly connected to the opening of the supraorbital canal that is formed by the frontal. The tubular portion of the pterotic forms a canal enclosing the cephalic lateral line system. The deeper part, forming the basis for the tubular portion, slightly overlaps with the surrounding bones. Posteriorly, the pterotic bears the posterior suspensorial articulatory facet. The posterior border of the pterotic passes slightly the posterior margin of the supraoccipital. The sphenotic is directed ventroanteriorly and bears an extensive sphenotic process (Fig. 2A and B). Medially, the sphenotic process bears the lateral part of the anterior suspensorial articulatory facet. The large parietals are fused and are situated posteriorly against the frontal. The frontal ridge is continuous with a parietal ridge in the midline. This ridge is the origin of the A2βp and A2βa subsections of the adductor mandibulae muscle complex, which passes laterally over the parietal and hyomandibula. The prootics form the anterior part of the otic bullae. The posterior end of the prootics is attached to the basioccipital and laterally attaches to the pterotic (Fig. 2B). The posterior rim of the pterosphenoid is covered by the anterior rims of two prootic bones and these two bones meet each other in the midline above the parasphenoid (Fig. 2B). The suture between the basioccipital and prootic is interdigitating (Fig. 2B). The jugular foramen is present on the anterior part of the prootic (Fig. 2B). The trigemino-facial foramen is situated posterior to the jugular foramen (Fig. 2B). The epiotics (epioccipitals) form the posterodorsal face of the cranium and medially contact the supraoccipital (Fig. 2A).

The occipital region is composed of the supraoccipital, exoccipitals and basioccipital. These bones form the posterior wall of the neurocranium. The supraoccipital is surrounded by the epiotics (epioccipitals), parietal and exoccipitals and bears a small median crest (Fig. 2A). Caudally, the exoccipitals are domed and dorsally border the foramen magnum. Also, they ventrally connect to the basioccipital. The well-developed occipital condyle of the basioccipital forms the posterior end of the neurocranium and forms the ventral margin of the foramen magnum. The basioccipital extends anteriorly to the posterior border of the prootics and forms the posterior part of the otic bullae.
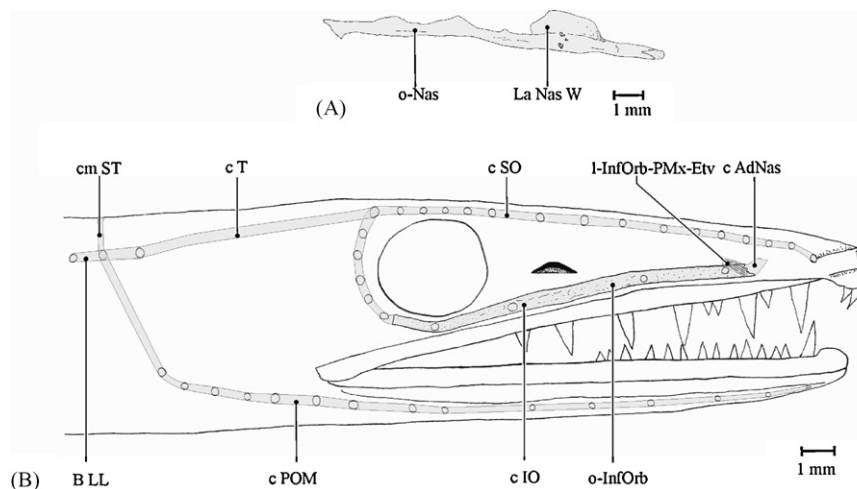


**Fig. 4.** The cranial lateral line system of *H. punctata*. (A) Lateral view of the canals (right side). Circles show external sensory pores. (B) Dorsal view of the left nasal bone. *Abbreviations*: B LL, body lateral line system; c AdNas, adnasal canal; c IO, infraorbital canal; c POM, preopercular mandibular canal; c SO, supraorbital canal; c T, temporal canal; cm ST, supratemporal commissure; La Nas W, lateral nasal wings; l-InfOrb-PMx-Etv, infraorbito-premaxillo-ethmovomeral ligament; o-InfOrb, infraorbital; o-Nas, nasal.

The nasal, a long bone, possesses a broad wing at the rear of its tip (Fig. 4A). It encloses the anterior part of the supraorbital canal. The infraorbital is a long, tube-shaped bone. The infraorbito-premaxillo-ethmovomeral ligament connects the anterior end of the infraorbital bone to the premaxillo-ethmovomeral complex. Furthermore, the maxillo-premaxillo-ethmovomero-infraorbital ligament connects the posterior end of the infraorbital bone to the posterodorsal side of the maxillary. The infraorbital bone encloses the body of the infraorbital canal and its posterior part curves dorsally (Fig. 4B).

The maxillary is ankylosed anteromedially to the premaxillo-ethmovomeral complex (Fig. 3A). The primordial ligament connects the posterior edge of the maxillary to the posterolateral face of the mandibular (Fig. 5A). The maxillo-premaxillo-ethmovomero-infraorbital ligament connects the posterodorsal face of the maxillary to the posterior part of the infraorbital bone and the posterior part of the ventral crest of the premaxillo-ethmovomeral complex (Fig. 5A). The maxillary bears a row of small, pointed teeth on its anterior half and a double row of smaller teeth on its posterior half (Fig. 6A). The lower jaw is slightly shorter than the upper jaw (Fig. 3A). The dentary is elongated and its coronoid process is connected to the angular complex. The mandibular teeth are arranged in two rows, with the medial row comprising caniniform teeth that are larger than the ones in the lateral row (Fig. 6B). The angular complex consists of the fused angular and articular, bearing a small retroarticular process. The angular complex possesses a posterior process behind the Meckelian fossa (Fig. 6B). The retroarticular process is directed caudomedially.

The suspensorium is composed of five elements: the hyomandibula, quadrate, palatopterygoid, preopercle and a cartilaginous element that may correspond to a non-ossified pars symplectic of the hyosymplictic (Fig. 3B). The preopercle is described as part of the opercular series (see below). The cartilaginous element of the suspensorium is situated ventral to the hyomandibula (Fig. 3B). The hyomandibula and quadrate are closely connected and form a solid structure. The hyomandibula articulates dorsally with the neurocranium via two articular condyles. The anterior one fits into a socket formed by the sphenotic and pterotic, whereas the posterior one fits into a facet on the pterotic. The lateral face of the suspensorium has an elevated ridge for the origin of the A2αv and A3 subsections of the adductor mandibulae muscle complex and insertion of the levator arcus palatine muscle. The opercle articulates with a condyle on the posterior edge of the hyomandibula (Fig. 3B). The palatopterygoid is attached to the anterior edge of the quadrate by connective tissue, and it is firmly connected to the lateral face of the premaxillo-ethmovomeral complex, at the caudal face of the maxillo-ethmovomeral articulation facet. The palatopterygoid ligament also connects the suspensorium to the palatopterygoid (Fig. 3B).

The opercular series is composed of four bones: the preopercle, interopercle, subopercle and opercle (Fig. 7A). The distal margins of the opercular bones were lightly stained in the specimens studied. The medial face of the anterior process of the preopercle is connected to the lower jaw through the angulo-preopercular ligament. The two preopercular pores are present on the dorsal rim and the anterior process of the preopercle, respectively. The interopercle is triangular in shape and is covered laterally by the posterior portion of the preopercle. The interopercle is connected to the angular complex via the angulo-interopercular ligament. The subopercle abuts against the caudal edge of the interopercle and curves along the entire posterior margin of the opercle. The subopercle is attached to the opercle by connective tissue. The fan-shaped opercle articulates with the opercular condyle of the hyomandibula through its anterior process (Fig. 3B). The operculo-interopercular ligament connects the medial face of the anterior process of the opercle to the dorsomedial face of the interopercle (Fig. 3B).
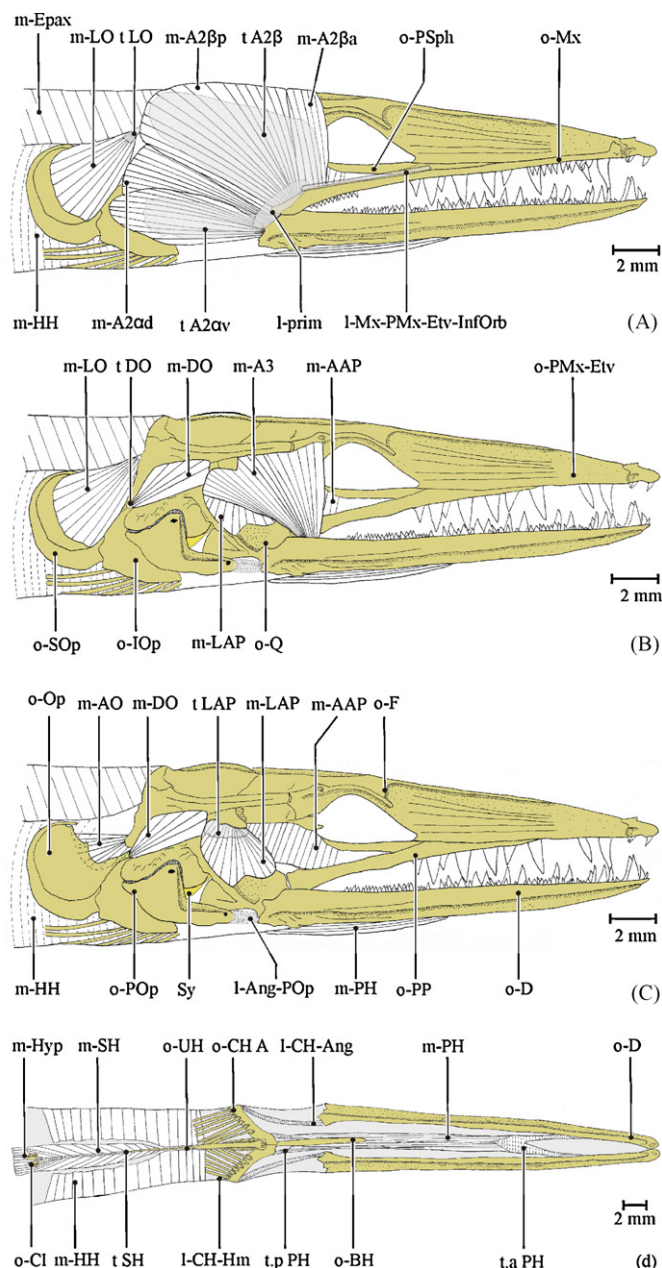


Fig. 5. Lateral view of the cranial muscles of *H. punctata*. (A) Skin removed; (B) primordial ligament and subsections of A2, with exception of A2βd, removed; (C) A2βd and A3 removed; (D) ventral view of the cranial muscles (with skin removed). *Abbreviations*: l-Ang-POp, angulo-preopercular ligament; l-CH-Ang, ceratohyalo-angular ligament; l-CH-Hm, ceratohyalo-hyomandibular ligament; l-Mx-PMx-Etv-InfOrb, maxillo-premaxillo-ethmovomero-infraorbital ligament; l-prim, primordial ligament; m-A1, A1 section of the adductor mandibulae muscle complex; m-A2, A2 section of the adductor mandibulae muscle complex; m-A2α, ventral subsection of A2; m-A2αd, dorsal subsection of A2α; m-A2αv, ventral subsection of A2α; m-A2β, dorsal subsection of A2; m-A2βa, anterior subsection of A2β; m-A2βp, posterior subsection of A2β; m-A3, A3 section of the adductor mandibulae muscle complex; m-AAP, adductor arcus palatini muscle; m-AO, adductor operculi muscle; m-DO, dilatator operculi muscle; m-Epax, epaxial muscles; m-HH, hyohyoideus muscle; m-Hyp, hypaxial muscles; m-LAP, levator arcus palatini muscle; m-LO, levator operculi muscle; m-PH, protractor hyoidei muscle; m-SH, sternohyoideus muscle; o-BH, basihyal; o-CH A, anterior ceratohyal; o-Cl, cleithrum; o-D, dentary; o-F, frontal; o-IOp, interopercle; o-Mx, maxillary; o-PMx-Etv, premaxillo-ethmovomeral complex; o-Op, opercle; o-POp, preopercle; o-PP, palatopterygoid; o-PSph, parasphenoid; o-Q, quadrate; o-SOp, subopercle; o-UH, urohyal; t A2αv, tendon of A2αv; t A2β, tendon of A2β; t DO, tendon of dilatator operculi; t LAP, tendon of levator arcus palatini; t LO, tendon of levator operculi; t.a PH, anterior tendon of protractor hyoidei; t.p PH, posterior tendon of protractor hyoidei; t SH, tendon of sternohyoideus.
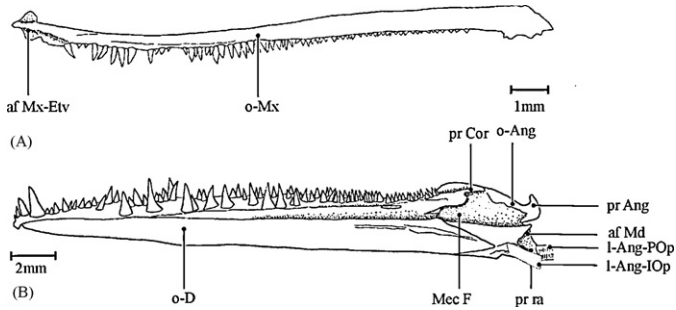
**Fig. 6.** Jaw of *H. punctata* (right side, medial view); (A) lower jaw, (B) maxillary. *Abbreviations*: af Md, mandibular articulation facet; af Mx-Etv, maxillo-ethmovomerine articulation facet; l-Ang-IOp, angulo-interopercular ligament; l-Ang-POp, angulo-preopercular ligament; o-Ang, angular complex; o-D, dentary; o-Mx, maxillary; Mec F, Meckelian fossa; pr Ang, angular process; pr Cor, coronoid process; pr ra, process of retroarticular.

The hyoid complex consists of the unpaired, long cylindrical basihyal, spatulate urohyal, paired anterior ceratohyals and paired posterior ceratohyals (Fig. 7B and C). The posterior part of the urohyal expands vertically and is blade-like in its lateral aspect. The anterior ceratohyals are the largest elements of the hyoid arch and articulate with the urohyal. The anterior ceratohyal is interdigitated posteriorly with the posterior ceratohyal. Two of seven branchiostegal rays are connected to the anterior ceratohyal and the others to the posterior ceratohyal. The branchiostegal rays curve dorsally along the ventral border of the interopercle. They reach up to the caudal border of the subopercle. The posterior ceratohyals are connected to the suspensorium and angular complex by two ceratohyalo-hyomandibular and ceratohyalo-angular ligaments, respectively (Fig. 7C).

### 3.2. Cephalic lateral line system

The cephalic lateral line system is composed of the supraorbital canal, adnasal canal, infraorbital canal, temporal canal, preoperculo-mandibular canal and supratemporal commissure. The supraorbital canal extends from the tip of the snout to the interorbital region, and bears fourteen pores. The adnasal canal, a short ascending branch of the infraorbital canal, starts at the rear of the anterior nostril. The infraorbital canal curves dorsally into the postorbital region. This canal bears four pores exiting from

the infraorbital bone and five pores on the postorbital region. The preoperculo-mandibular canal starts almost from the rostral tip of the dentary and its anterior part runs in an inferior crest of the dentary. This canal curves dorsally into the postorbital region and enters into the posterior end of the temporal canal (Fig. 4B). The supratemporal commissure connects the right and left cephalic lateral line system. No ethmoid canals were observed.

### 3.3. Myology of H. punctata

The large adductor mandibulae muscle complex comprises the sections A2 and A3. Despite a small and indirect connection between tendon A2αv and the maxillary via the primordial ligament (which could suggest a homology with A1), this subsection was termed A2αv based on the terminology of Winterbottom (1974) and due to its main insertion being onto the posteromedial face of the lower jaw (Fig. 5A). Section A2 can be subdivided into four subsections: A2β anterior, A2β posterior, A2α dorsalis and A2α ventralis (Fig. 5A). Subsection A2βp is the largest portion of the adductor mandibulae muscle complex and originates musculously from the supraoccipital, epiotic (epioccipital), parietal and frontal. It inserts tendinously onto the dorsomedial edge of the coronoid process and the anterior portion of the Meckelian fossa. Subsection A2βa originates musculously from the frontal and parietal, and inserts tendinously onto the medial face of the coronoid process. The posterior portion of subsection A2βa lies medial to the anterior portion of subsection A2βp. The subsections A2βa and A2βp are attached laterally to a single tendon of A2β. Subsection A2αd originates musculously from the posterolateral face of the hyomandibula and the posteroventral face of the pterotic. It inserts tendinously onto the dorsomedial edge of the angular complex. The superficial portion of subsection A2αv originates musculously from the anterolateral face of the preopercle, with its medial fibers attaching musculously to the hyomandibula and quadrate. Subsection A2αv inserts through a tendon onto the posteromedial face of the angular process and musculously on the medial face of this process. An Aω was not observed.

The section A3 is situated medial to the subsection A2β and covers the dorsolateral face of the levator arcus palatini muscle and the posterior portion of the adductor arcus palatini muscle (Fig. 5B). This section originates musculously from the lateral ridge of the hyomandibula, the ventral face of the sphenotic, the anteroventral face of the pterotic, the dorsolateral side of the pterosphenoid and
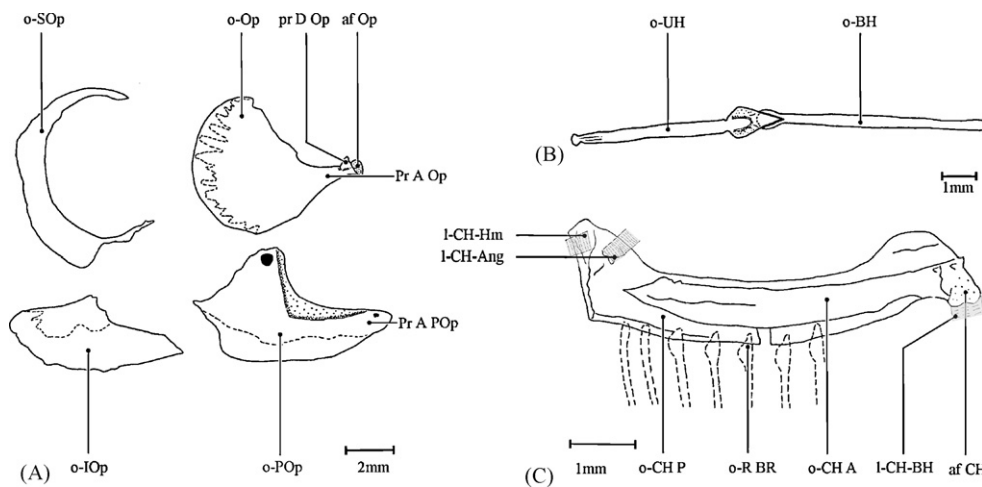


**Fig. 7.** Hyoid and opercular series of *H. punctata*. (A) Dorsal view of the basihyal and urohyal; (B) the anterior and posterior ceratohyal in medial view (right side); (C) the opercular series in lateral view (right side). *Abbreviations*: af CH, ceratohyal articular facet; af Op, opercular articular facet; l-CH-Ang, ceratohyalo-angular ligament; l-CH-BH, ceratohyalo-basihyal ligament; l-CH-Hm, ceratohyalo-hyomandibular ligament; o-BH, basihyal; o-CH A, anterior ceratohyal; o-CH p, posterior ceratohyal; o-IOp, interopercle; o-Op, opercle; o-POp, preopercle; o-SOp, subopercle; o-R BR, branchiostegal rays; o-UH, urohyal; pr A Op, anterior process of opercle; pr A POp, anterior process of preopercle; pr D Op, dorsal process of anterior process of opercle.

the posteroventral face of the frontal's lateral expansion. It inserts tendinously into the Meckelian fossa. Section A3 slightly bulges laterally at the level of its vertical midline.

The levator arcus palatini muscle originates musculously and tendinously from the ventral face of the sphenotic process and the dorsolateral faces of the prootic (Fig. 5C). This muscle bulges slightly in the midline. It inserts musculously on the anterior face of the lateral ridge and the ventrolateral face of the hyomandibula.

The adductor arcus palatini muscle originates from the ventrolateral face of the parasphenoid, the ventrolateral face of the basisphenoid, the ventral face of the pterosphenoid and the anterolateral face of the prootic (Fig. 5C). It fills the posterior part of the fissura infraorbitalis and inserts musculously on the caudomedial surface of the palatopterygoid and the medial face of the hyomandibula. A thick posterior portion of the adductor arcus palatini muscle could be discriminated based on a discrete change in thickness from an anterior thin part, but with the two parts still forming a continuous muscle sheet. The thicker portion of the adductor arcus palatini muscle runs up to the medial face of the hyomandibula. The fibers of the posterior part of the adductor arcus palatini muscle take up the position where the adductor hyomandibulae muscle would be found.

The levator operculi muscle originates tendinously from the caudal margin of the pterotic. Its fibers are directed caudoventrally and diverge, inserting musculously on the dorsal part of the lateral face of the opercle (Fig. 5A and B).

The adductor operculi muscle originates musculously from both the posterior part of the pterotic and the exoccipital. Proximally, its fibers run continuously with the fibers of the levator operculi muscle but insert on the dorsomedial surface of the opercle (Fig. 5C).

The dilatator operculi muscle is situated posterior to the levator arcus palatini muscle and the section A3. The dilatator operculi muscle is a triangular muscle, with the apex pointing caudoventrally (Fig. 5B). This muscle originates musculously from the posteroventral face of the sphenotic and the posterolateral face of the pterotic. The dilatator operculi muscle inserts tendinously on the small process which is situated on the dorsal side of the anterior process of the opercle (Fig. 5C and 7A).

Two separate halves (right and left) of the protractor hyoidei muscle connect the lower jaw to the hyoid arch. Each of these portions originates tendinously from the medial face of the dentary at the rear of the dentary symphysis and inserts by means of a tendon on the dorsal surface of the posterior ceratohyal (Fig. 5D).

The sternohyoideus muscle originates musculously from the lateral surface and tendinously from the anteroventral face of the cleithrum, with some of its fibers merging with those of the hypaxial musculature. The sternohyoideus is a bipinnate muscle and the posterior fibers of the left and right halves attach via a central tendon on the posterior end and the ventral face of the urohyal. The anterior fibers of the left and right halves of the sternohyoideus muscle attach musculously on the lateral sides of the posterior part of the urohyal (Fig. 5D).

The hyohyoideus muscle complex in teleosts generally comprises three components: the hyohyoideus inferioris, hyohyoideus abductor and the hyohyoidei adductors. However, in *H. punctata* these muscles are undifferentiated and merged as a thin sac-like muscle sheet meeting its counterparts at the ventral midline. The ventral fibers of the hyohyoideus muscle complex attach to the dorsal face of the branchiostegal rays. This sac-like muscle connects to the medial face of the opercle and reaches dorsally up to the horizontal septum.

The epaxial musculature attaches to the exoccipitals, pterotics and supraoccipital. The hypaxial musculature attaches to the basioccipital.

### 3.4. Shape comparison

The deformation grids from *C. conger* and *H. hassi* to *H. punctata* clearly show a distinct elongation of the preorbital region, including the rostral region, maxillary and lower jaw (Fig. 8). Furthermore, the jaw elongation results in the quadrate–mandibular articulation being positioned well posterior in *H. punctata* and *C. conger*, up to the posterior region of the orbit, whereas this joint is situated at the midpoint of the orbit in *H. hassi*. The deformation grids also indicate a more dorsal position of this articulation, reflecting a relative decrease in the depth of the suspensorium in *H. punctata* compared to the other two. The same decrease in depth is also observed in the neurocranium.

The distance between the anterior suspensorial facet and the posterior end of the orbit is larger in *H. punctata* due to a reduction of the orbit size and a backward displacement of the hyomandibula. The anterior end of the pterotic is extended substantially in *C. conger* and forms a small shelf over the posterior part of the orbit, but in *H. punctata* and *H. hassi* it is situated in the postorbital region. Such a shelf is absent in *H. hassi* and is rather formed by the lateral expansion of the frontal in *H. punctata*. The opercle–hyomandibular joint
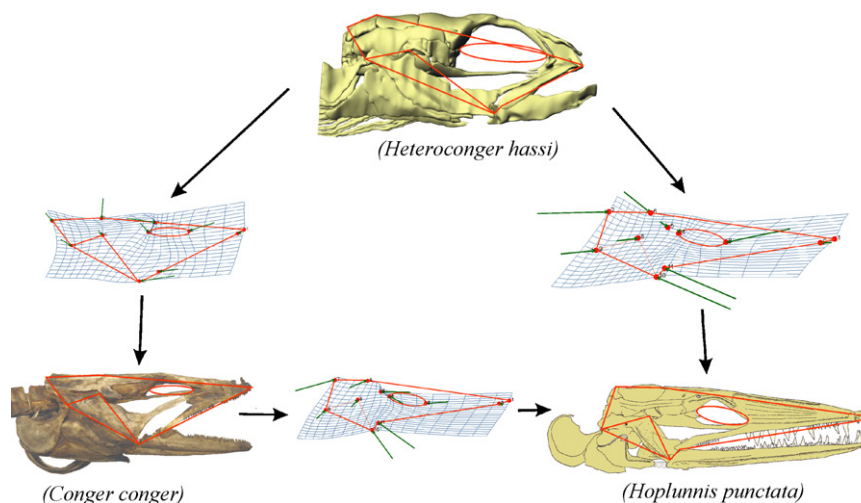


**Fig. 8.** Cranial shape comparison between *Hoplunnis punctata*, *Conger conger* and *Heteroconger hassi*: the deformation grids show shape differences, especially in jaw elongation, when moving from a species with a shorter jaw toward a species with a longer one (in the direction as indicated by the arrows). The lengths of the arrows in the grids represent the shifts in homologous landmark positions among the three studied species.

is also positioned caudal to the posterior edge of the neurocranium in *H. punctata* (Fig. 8).

## 4. Discussion

### 4.1. Morphological changes in relation to jaw elongation

*H. punctata* and *C. conger* are active predators, whereas *H. hassi* lives in burrows and projects the front portion of the body from the burrow to feed on zooplankton (Casimir and Fricke, 1971; Smith, 1989b). *C. conger* is a nocturnal predator feeding on fishes, crustaceans and cephalopods (Bauchot and Saldanha, 1986). *H. hassi* feeds on the plankton-loaded currents by snapping and picking small zooplanktonic particles (Smith, 1989b; Vigliola et al., 1996; Castle and Randall, 1999; De Schepper et al., 2007), whereas *H. punctata* is a benthic fish and feeds on small fishes and invertebrates (Smith, 1989a).

Comparison of morphological structures with different configurations, particularly in a phylogenetic context, may contribute to the proper understanding of morphological evolutionary changes within functional units. Hence, the morphological differences of the heads of the representatives with long (*H. punctata*), moderate (*C. conger*) and short (*H. hassi*) jaw lengths used in this study may allow a better understanding of the morphological changes in relation to the elongation of the rostral region and jaws.

#### 4.1.1. Osteology

The long preorbital region of *H. punctata* and the moderate one in *C. conger* differ in shape from that of *H. hassi* which possesses a particularly short one (Fig. 8). The frontals of *H. punctata*, *C. conger* and *H. hassi* are fused into a single unit, just as in the Derichthyidae (Robins, 1989) and Muraenesocidae (Smith, 1989c), which is considered a derived character in Anguilliformes (Belouze, 2001). There is no frontal shelf over the eyes and no frontal ridge in *H. hassi* and *C. conger*, unlike in *H. punctata*. The parietals have not fused in *C. conger* and *H. hassi*, but a fusion is observed in *H. punctata*. The fusion of the parietals is a unique character state within the Anguilliformes (Belouze, 2001). The conical mandibular and vomeral teeth of *H. punctata* are large and sharp, whereas those of *H. hassi* are small. The teeth of the upper and lower jaws in *C. conger* are arranged in a double row, with big incisiform outer teeth and small inner ones. The posterior edge of the supraoccipital crest does not reach the posterior edge of the skull in *H. punctata* while that of *C. conger* reaches beyond the posterior edge of the skull. This crest is absent in *H. hassi*. Absence of the supraoccipital crest is a plesiomorphic condition which is seen in fossil Anguilliformes (Belouze, 2001).

The quadrate and hyomandibula of *H. punctata* and *C. conger* are strongly interconnected and form a solid structure. In *H. hassi*, these two bones seem slightly mobile with respect to each other, since they move somewhat when pressed by forceps. There is no symplectic in *C. conger*, but a cartilaginous element is present posterior to the quadrate in *H. hassi* and ventral to the hyomandibula in *H. punctata* where the symplectic would be found if present. A posterocaudal process of the subopercle is connected to the posterior border of the opercle in *H. punctata* and *C. conger*, while in *H. hassi* this process is lacking.

#### 4.1.2. Myology

The adductor mandibulae muscle complex of *H. punctata* and *C. conger* is greatly enlarged compared to that of *H. hassi*. De Schepper et al. (2007) mentioned that the expansion of the adductor mandibulae muscle of *H. hassi* may have been restricted by its large eyes. The adductor mandibulae muscle complex comprises sections A2 (with one subsection), A3 and Aω in *H. hassi*. In *C. conger*, a medial subsection A2β and a lateral subsection A2α are found, as well as two subsections of A3 that insert on the medial
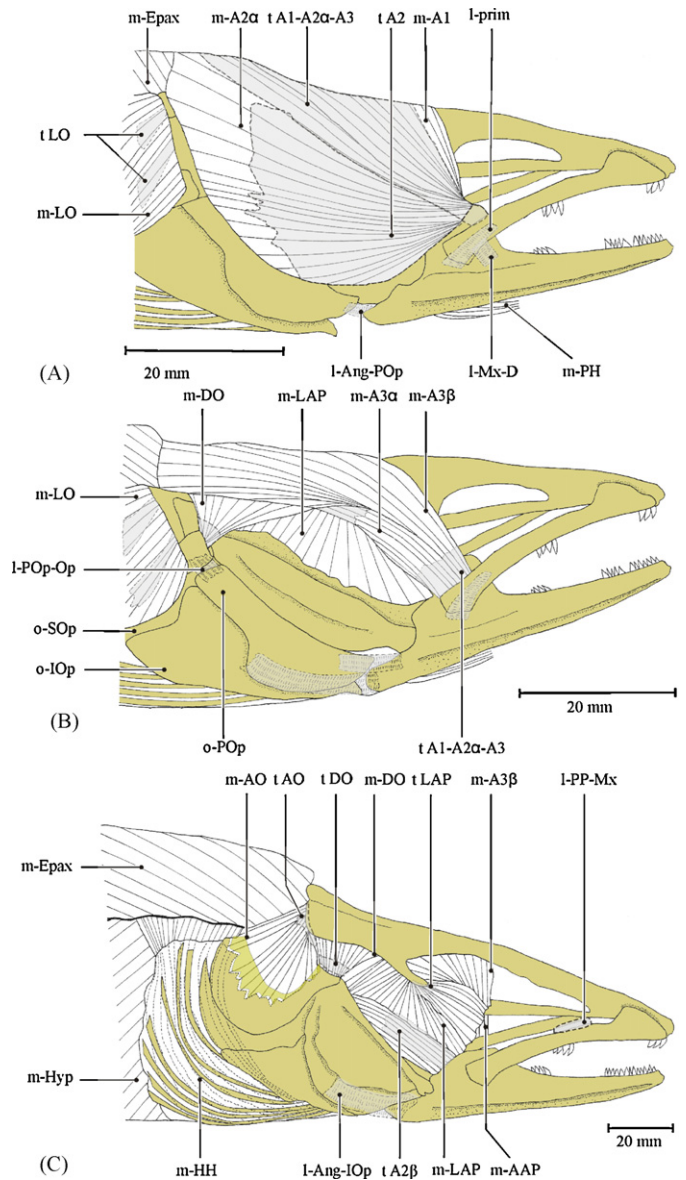


**Fig. 9.** Lateral view of the cranial muscles of *C. conger* (modified after De Schepper, 2007). (A) Skin removed; (B) primordial ligament and subsections of A2 except A2βd removed; (C) lateral view of the cranial muscles after removing skin, A1, A2, and A3 muscles. *Abbreviations*: l-Ang-POp, angulo-preopercular ligament; l-Ang-IOp, angulo-interopercular ligament; l-Mx-D, maxillo-dentary ligament; l-POp-Op, preoperculo-opercular ligament; l-PP-Mx, palatopterygoideo-maxillar ligament; l-prim, primordial ligament; m-A1, A1 section of the adductor mandibulae muscle complex; m-A2α, ventral subsection of A2; m-A3, A3 section of the adductor mandibulae muscle complex; m-A3α, ventral subsection of A3; m-A3β, dorsal subsection of A3; m-AAP, adductor arcus palatini muscle; m-AO, adductor operculi muscle; m-DO, dilatator operculi muscle; m-Epax, epaxial muscles; m-HH, hyohyoideus muscle; m-Hyp, hypaxial muscles; m-LAP, levator arcus palatini muscle; m-LO, levator operculi muscle; m-PH, protractor hyoidei muscle; o-IOp, interopercle; o-POp, preopercle; o-SOp, subopercle; t A1-A2α-A3, tendon of t A1-A2α-A3; t A2, tendon of A2; t A2β, tendon of A2β; t AO, tendon of adductor operculi; t DO, tendon of dilatator operculi; t LAP, tendon of levator arcus palatini; t LO, tendon of levator operculi.

face of the mandibular by a single tendon (Fig. 9). The Aω section of the adductor mandibulae muscle, which is found in most major osteichthyan groups (Diogo et al., 2008), is absent in some species in all groups within the Teleostei (Nakae and Sasaki, 2004; Hertwig, 2008). Hence, the presence of section Aω in *H. hassi* may be a retained plesiomorphic character, but in the current absence of additional myological data of other anguilliform taxa, this needs to

be confirmed. The presence of an intermandibularis muscle and a differentiated hyohyoideus inferioris muscle are two features in *H. hassi* that are not found in *H. punctata* and *C. conger*. The shape comparison of the skull of the three species studied shows a relatively horizontal and vertical stretching of the suspensorium and postorbital region in *H. hassi*. In relation to this stretching, the adductor arcus palatini muscle in *H. hassi* is prolonged rostrally up to the anterior portion of the orbit.

The adductor hyomandibulae is present as a separate muscle in *H. hassi*. This muscle has been reported in *C. conger* by De Schepper (2007), lying medial to the adductor arcus palatini muscle. It has been described as "difficult to distinguish" (De Schepper, 2007). It seems that this muscle has a configuration similar to the one described here for *H. punctata*. It is, therefore, morphologically an adductor hyomandibulae. In generalized lower teleosts, such as Osteoglossomorpha, Elopomorpha and Elupeomorpha, the adductor arcus palatini connects the prootic to the dorsomedial face of the hyomandibula (Winterbottom, 1974). Based on Winterbottom (1974), the term adductor arcus palatini is applied to a muscle that has expanded anteriorly along the floor of the orbit, as is seen in *H. punctata* and *C. conger*, and an adductor hyomandibulae muscle is only distinguished by the presence of a separate anterior adductor arcus palatini muscle.

### 4.1.3. Jaw elongation

Substantial differences in the length of the rostral region and the jaw can be observed between representatives of the monophyletic group comprising the Heterocongrinae-Derichthyidae clade (clade A) and the Congrinae-Muraenesocidae-Nettastomatidae clade (clade B) (Fig. 1). The members of clade A possess a short to moderate preorbital region including the rostral region and jaws and those of clade B a moderate to long one, as seen in *H. punctata*. In clade B, especially Muraenesocidae and Nettastomatidae possess a substantially elongated rostral region and jaws (Smith, 1989c).

Regarding the plesiomorphic condition of a short rostral region of the Anguilliformes (Belouze, 2001), as is seen in many Anguilliformes, and considering the phylogenetic relationship of the Congrinae, Muraenesocidae and Nettastomatidae (Robins, 1989; Smith, 1989a; Wang et al., 2003; Obermiller and Pfeiler, 2003; Lopez et al., 2007), the elongation of the rostral region in clade B should be considered a derived character.

The presence of a median (i.e. fused) premaxillary in *Derichthys serpentinus* (Derichthyidae), a member of clade A, is a unique attribute among the Anguilliformes. Robins (1989) mentioned the trend in Derichthyidae towards a fusion of the premaxillaries with the ethmoid to form the premaxillo-ethmovomeral complex. Some derichthyid species such as *Nessorhamphus ingolfianus* bear a moderately long snout with the premaxillaries fused to the ethmoid (Robins, 1989). Furthermore, *H. hassi* possesses a very short rostral region, which does include a premaxillo-ethmovomeral complex. Differences in the preorbital elements of clade A and B indicate that the formation of a premaxillo-ethmovomeral complex in clade A should not be considered as reflecting the ancestral condition leading towards the elongation of the rostral region in clade B. Hence, based on parsimony, it would be easy to conceive an evolutionary trend toward a separation of the premaxillary from a premaxillo-ethmovomeral complex in *D. serpentinus*.

Furthermore, the shape comparison of the three species studied clearly shows the posterior position of the quadrate–mandibular articulation up to the postorbital region, which is an additional structural coupling to the jaw elongation.

### 4.2. Functional considerations of jaw elongation

The observed differences in the feeding apparatus of these anguilliforms, especially those related to jaw elongation, can be considered to have a potential influence on the functionality of this apparatus. However, this would require performance testing to empirically support this hypothesis (Arnold, 1983). Still, some hypotheses can be derived from the observed morphology.

The maxillary in *H. punctata* is connected firmly to the premaxillo-ethmovomeral complex along most of its length, while in *H. hassi* only the anterior portion of the maxillary is resting on this bony complex. This configuration of the maxillary in *H. hassi*, combined with the forward position of the quadrate–mandibular joint, results in a small and more oblique mouth border, which has been regarded as a specialization for snapping planktonic prey (Rosenblatt, 1967). This specialization in *H. hassi* may then compensate for the lack of upper jaw protrusion due to the immobility of the premaxillary (which is fused to the ethmoid and vomer). In contrast to the forward position of the quadrate–mandibular joint of *H. hassi*, the one in *H. punctata* is positioned posterior to the orbit and results in a large mouth with a longer lower jaw that may allow rapid mouth closing (see below).

The relatively narrow and low skull of *H. punctata* implies a shallow orobranchial chamber, which along with its immobile, long maxillaries suggests that food may be obtained by biting rather than by filtering or engulfing through suction feeding (Schaeffer and Rosen, 1961). Fishes that rely on high-velocity lunges followed by biting rather than suction exhibit longer strike times (Porter and Motta, 2004; Mehta and Wainwright, 2007), and benthic biters are typically slower than suction feeders (Alfaro et al., 2001; Rice and Westneat, 2005; Konow and Bellwood, 2005). Biting may represent an important behavioral adaptation enabling predators to subdue large prey (Mehta and Wainwright, 2007). It is thus not surprising to find a wide range of morphologically diverse biters (Westneat, 2004; De Schepper et al., 2008; Grubich et al., 2008; Mehta, 2009).

The strongly developed adductor mandibulae muscle complex of *H. punctata* and *C. conger*, compared to a rather small one in *H. hassi*, also suggests that their prey capturing mode is biting. Enlarged adductor mandibulae muscles may allow a powerful bite by increasing the mechanical load on skeletal elements such as dentaries, suspensoriums and neurocranium (Herrel et al., 2002; Van Wassenbergh et al., 2004). A predatory life style is considered the plesiomorphic condition for the Anguilliformes (Gosline, 1971; Smith, 1989b), with hypertrophied jaw muscles being common (Böhlke et al., 1989).

The maxillaries of the Anguilliformes are tightly joined to the cranium and are immobile or can move very little (Eaton, 1935). Hence, the lower jaw is considered the sole contributor to jaw rotation, with the quadrate–mandibular joint working as a fulcrum (Alexander, 1967; Westneat, 2004). Based on the velocity advantage (small input/output lever ratio), a long lower jaw may result in faster mouth closing (higher biting speed), which would be an advantage for a predator feeding on elusive prey. Simultaneously, this low ratio also implies a lower mechanical advantage. Hence, having a high input force generated by enlarged adductor mandibulae muscles, as seen in *H. punctata* and *C. conger*, can compensate for this deficiency and produce sufficiently high biting forces during snapping movements.

Elongation of the rostral region can provide more space for the olfactory rosette in benthic *H. punctata*, which is also substantially large. Related to this, an improved olfaction would benefit their predatory life style to detect prey. The size of the rosette is proportional to the fish's ability to smell, and the broadly spaced nares provide a significantly greater separation between the olfactory rosettes, which could lead to an enhanced ability to resolve odor gradients (Kajiura et al., 2005).

Elongation of the preorbital region including the rostral region and jaws such as in *H. punctata* may also provide a hydrodynamic advantage for drag reduction during feeding strikes and swimming.

Fish (1998) pointed out that departure from a smoothly rounded head in a number of aquatic animals that have projecting beaks, bills, and rostrums, may be related to a better functioning of their feeding morphology requiring grasping jaws. The alternatingly concave and convex profile of the anterior part of the body, which is seen in aquatic animals with projecting anterior structures, may induce a stepwise, gradual drag pressure change that can reduce skin friction in animals during swimming (Bandyopadhyay, 1989; Bannasch, 1995; Bandyopadhyay and Ahmed, 1993). The relatively small surface area of the anterior projection can also decrease drag, due to a reduced pressure gradient during swimming (Kramer, 1960; Videler, 1995).

The cranial anatomy of *H. punctata* shows a number of different features compared to the studied short-snouted species, which may be related to the observed elongation of the snout. Also, some features may reflect differences in prey capturing behavior, such as large and sharp piercing teeth on the pars vomeralis and the mandibular bones, the depth and anterior reduction in depth and anterior length of the suspensorium, enlarged adductor mandibulae muscle complex, reduction of neurocranium depth and posterior position of the quadrate–mandibular joint. The jaw elongation can confer some advantages such as providing more space for the olfactory rosette, increasing velocity advantage (biting speed) and reducing drag, thus improving the prey capture kinematics of this benthic biter predator.

## Acknowledgments

## References

Alexander, R.McN., 1967. The functions and mechanisms of the protrusible upper jaws of some acanthopterygian fish. J. Zool. Lond. 151, 43–64.
Alfaro, M.E., Janovetz, J., Westneat, M.W., 2001. Motor control across trophic strategies: muscle activity of biting and suction feeding fishes. Am. Zool. 41, 1266–1279.
Arnold, S.J., 1983. Morphology, performance and fitness. Am. Zool. 23, 347–361.
Bandyopadhyay, P.R., 1989. Viscous drag reduction of a nose body. AIAA J. 27, 274–282.
Bandyopadhyay, P.R., Ahmed, A., 1993. Turbulent boundary layers subjected to multiple curvatures and pressure gradients. J. Fluid Mech. 246, 503–527.
Bannasch, R., 1995. Hydrodynamics of penguins – an experimental approach. In: Dann, P., Norman, I., Reilly, P. (Eds.), The Penguins: Ecology and Management. Surrey Beatty and Sons, Norton, pp. 141–176.
Bauchot, M.-L., Saldanha, L., 1986. Congridae (including Heterocongridae). In: Whitehead, P.J.P., Bauchot, M.-L., Hureau, J.-C., Nielsen, J., Tortonese, E. (Eds.), Fishes of the North-eastern Atlantic and the Mediterranean, 2. UNESCO, Paris, pp. 567–574.
Belouze, A., 2001. Compréhension morphologique et phylogénétique des taxons actuels et fossils rapports aux Anguilliformes (Poissons, Téléostéens). Ph.D. Thesis. Université Claude Bernard Lyon 1.
Bock, W.J., Shear, R.C., 1972. A staining method for gross dissection of vertebrate muscles. Anat. Anz. 130, 222–227.
Böhlke, E.B., 1989. Methods and terminology. In: Böhlke, E.B. (Ed.), Fishes of the Western North Atlantic. Sears Foundation for Marine Research, New Haven, pp. 1–8.
Böhlke, E.B., McCosker, J.E., Böhlke, J.E., 1989. Family Muraenidae. In: Böhlke, E.B. (Ed.), Fishes of the Western North Atlantic. Sears Foundation for Marine Research, New Haven, pp. 104–206.
Casimir, M.J., Fricke, H.W., 1971. Zur Funktion, Morphologie und Histochemie der Schwanzdrüse bei Röhrenaalen (Pisces, Apodes, Heterocongridae). Mar. Biol. 9, 339–346.
Castle, P.H.J., Randall, J.E., 1999. Revision of Indo-Pacific Garden Eels (Congridae: Heterocongrinae), with Descriptions of Five New Species, Indo-Pacific Fishes No. 30.
De Schepper, N., 2007. Evolutionary morphology of body elongation in teleosts: aspects of convergent evolution. Ph.D. Thesis. Ghent University.

De Schepper, N., Adriaens, D., De Kegel, B., 2005. *Moringua edwardsi* (Moringuidae: Anguilliformes): cranial specialization for head-first burrowing? J Morphol. 266, 356–368.
De Schepper, N., De Kegel, B., Adriaens, D., 2007. Morphological specialization in Heterocongrinae (Anguilliformes: Congridae) related to burrowing and feeding. J. Morphol. 268, 343–356.
De Schepper, N., Van Wassenbergh, S., Adriaens, D., 2008. Morphology of the jaw system in trichiurids: trade-offs between mouth closing and biting performance. Zool. J. Linn. Soc. 152, 717–736.
Diogo, R., Hinits, Y., Hughes, S.M., 2008. Development of mandibular, hyoid and hypobranchial muscles in the zebrafish: homologies and evolution of these muscles within bony fishes and tetrapods. BMC Dev. Biol. 8, 24, doi:10.1186/1471-213X-8-24.
Eaton Jr., T.H., 1935. Evolution of the upper jaw mechanism in teleost fishes. J. Morphol. 58, 157–172.
Ferry-Graham, L.A., Lauder, G.V., 2001. Aquatic prey capture in ray-finned fishes: a century of progress and new directions. J. Morphol. 248, 99–119.
Fish, F.E., 1998. Imaginative solutions by marine organisms for drag reduction. In: Meng, J.C.S. (Ed.), Proceedings of the International Symposium on Seawater Drag Reduction. Newport, Rhode Island, pp. 443–450.
Gosline, W.A., 1971. Functional Morphology and Classification of Teleostean Fishes. University Press of Hawaii, Honolulu.
Grubich, J., Rice, A.N., Westneat, M.W., 2008. Functional morphology of bite mechanics in the great barracuda (*Sphyraena barracuda*). Zoology 111, 16–29.
Hanken, J., Wassersug, R., 1981. The visible skeleton. A new double-stain technique reveals the nature of the "hard" tissues. Funct. Photogr. 16, 22–26.
Herrel, A., Adriaens, D., Verraes, W., Aerts, P., 2002. Bite performance in clariid fishes with hypertrophied jaw adductors as deduced by bite modelling. J. Morphol. 253, 196–205.
Hertwig, S.T., 2008. Phylogeny of the Cyprinodontiformes (Teleostei, Atherinomorpha): the contribution of cranial soft tissue characters. Zool. Scripta 37, 141–174.
Kajiura, S.M., Forni, B.J., Summers, A.P., 2005. Olfactory morphology of carcarhinid and sphyrnid sharks: does the cephalofoil confer a sensory advantage? J. Morphol. 264, 253–263.
Konow, N., Bellwood, D.R., 2005. Prey-capture in *Pomacanthus semicirculatus* (Teleostei, Pomacanthidae): functional implications of intramandibular joints in marine angelfishes. J. Exp. Biol. 208, 1421–1433.
Kramer, M.O., 1960. Boundary layer stabilization by distributed damping. J. Am. Soc. Nav. Eng. 72, 25–33.
Lauder, G.V., 1982. Pattern of evolution in the feeding mechanism of actinopterygian fishes. Am. Zool. 22, 275–282.
Lopez, J.A., Westneat, M.W., Hanel, R., 2007. The phylogenetic affinities of the mysterious anguilliform genera *Coloconger* and *Thalassenchelys* as supported by mtDNA sequences. Copeia 4, 959–966.
Mehta, R.S., 2009. Ecomorphology of the moray bite: relationship between dietary extremes and morphological diversity. Physiol. Biochem. Zool. 82, 90–103.
Mehta, R.S., Wainwright, P.C., 2007. Biting releases constraints on moray eel feeding kinematics. J. Exp. Biol. 210, 495–504.
Nakae, M., Sasaki, K., 2004. Homologies of the adductor mandibulae muscles in Tetraodontiformes as indicated by nerve branching patterns. Ichthyol. Res. 51, 327–336.
Obermiller, L.E., Pfeiler, E., 2003. Phylogenetic relationships of elopomorph fishes inferred from mitochondrial ribosomal DNA sequences. Mol. Phyl. Evol. 26, 202–214.
Patterson, C., 1975. The braincase of pholidophorid and leptolepid fishes, with a review of the actinopterygian braincase. Philos. Trans. R. Soc. Lond. B: Biol. Sci. 269, 275–579.
Porter, H.T., Motta, P.J., 2004. A comparison of strike and prey capture kinematics of three species of piscivorous fishes: Florida gar (*Lepisosteus platyrhincus*), redfin needlefish (*Strongylura notata*), and great barracuda (*Sphyraena barracuda*). Mar. Biol. 145, 989–1000.
Rice, A.N., Westneat, M.W., 2005. Coordination of feeding, locomotor and visual systems in parrotfishes (Teleostei: Labridae). J. Exp. Biol. 208, 3503–3518.
Robins, C.H., 1989. Family Derichthyidae. In: Böhlke, E.B. (Ed.), Fishes of the Western North Atlantic. Sears Foundation for Marine Research, New Haven, pp. 420–431.
Rohlf, F.J., 2004a. tpsSpline, Thin-Plate Spline, Version 1.16. Department of Ecology and Evolution, State University of New York at Stony Brook.
Rohlf, F.J., 2004b. tpsUtil, File Utility Program, Version 1.26. Department of Ecology and Evolution, State University of New York at Stony Brook.
Rohlf, F.J., 2005. tpsDig, Digitize Landmarks and Outlines, Version 2.08. Department of Ecology and Evolution, State University of New York at Stony Brook.
Rosenblatt, R.H., 1967. The osteology of the congrid eel *Gorgasia punctata* and the relationships of the Heterocongrinae. Pac. Sci. 21, 91–97.
Schaeffer, B., Rosen, D.E., 1961. Major adaptive levels in the evolution of the actinopterygian feeding mechanism. Am. Zool. 1, 187–204.
Smith, D.G., 1989a. Family Nettastomatidae. In: Böhlke, E.B. (Ed.), Fishes of the Western North Atlantic. Sears Foundation for Marine Research, New Haven, pp. 568–612.
Smith, D.G., 1989b. Family Congridae. In: Böhlke, E.B. (Ed.), Fishes of the Western North Atlantic. Sears Foundation for Marine Research, New Haven, pp. 460–567.
Smith, D.G., 1989c. Family Muraenesocidae. In: Böhlke, E.B. (Ed.), Fishes of the Western North Atlantic. Sears Foundation for Marine Research, New Haven, pp. 432–440.
Van Wassenbergh, S., Herrel, A., Adriaens, D., Aerts, P., 2004. Effects of jaw adductor hypertrophy on buccal expansion during feeding of air breathing catfishes (Teleostei, Clariidae). Zoomorphology 123, 81–93.

Verraes, W., 1981. Theoretical discussion on some functional-morphological terms and some general reflections on explanations in biology. Acta Biotheor. 30, 255–273.

Videler, J.J., 1995. Body surface adaptations to boundary-layer dynamics. In: Ellington, C.P., Pedley, T.J. (Eds.), Biological Fluid Dynamics. Society of Experimental Biology, Cambridge, pp. 1–20.

Vigliola, L., Galzin, R., Harmelin-Viven, M.L., Mazeas, F., Salvat, B., 1996. Hétérocongerina (Teleostei: Congridae). De la pente externe de Moorea (Il de la Société, Polynésie Française): distribution et biologie. Cybium 20, 379–393.

Wainwright, P.C., Bellwood, D.R., 2002. Ecomorphology of feeding in coral reef fishes. In: Sale, P.F. (Ed.), Coral Reef Fishes: Dynamics and Diversity in a Complex Ecosystem. Academic Press, San Diego, pp. 33–55.

Wainwright, P.C., Carroll, A.N., Collar, D.C., Day, S.W., Higham, T.E., Holzman, R.A., 2007. Suction feeding mechanics, performance, and diversity in fishes. Integr. Comp. Biol. 47, 96–106.

Wang, C.H., Kuo, C.H., Mok, H.K., Lee, S.C., 2003. Molecular phylogeny of elopomorph fishes inferred from mitochondrial 12S ribosomal RNA sequences. Zool. Scripta 32, 231–241.

Westneat, M.W., 2004. Evolution of levers and linkages in the feeding mechanisms of fishes. Integr. Comp. Biol. 44, 378–389.

Wilga, C.D., 2005. Morphology and evolution of the jaw suspension in lamniform sharks. J. Morphol. 265, 102–119.

Winterbottom, R., 1974. A descriptive synonymy of the striated muscles of the Teleostei. Proc. Acad. Nat. Sci. 125, 225–317.